Electrical Engineering (2026) 108:217
https://doi.org/10.1007/s00202-026-03561-w

ORIGINAL PAPER

Optimal cost analysis for 100% renewable energy integration in India: a step toward global electricity grid

Bimal Kumar Dora[1] · Sunil Bhat[1] · Arghya Mitra[1] · Damien Ernst[2] · Jing Dai[3,4] · Soumyabrata Das[1] · Raphael Fonteneau[2]

Received: 18 July 2025 / Accepted: 8 February 2026

Abstract
The rising global environmental challenges have highlighted the crucial requirement of renewable energy (RE) adoption as a core policy worldwide. India, endowed with abundant RE resources, has emerged as a pivotal contributor to the global clean energy transition. This study examines optimal investment strategies for solar, wind, battery storage, and energy imports to meet India's electricity demand. In this paper, three case studies are considered. The first is an isolated grid system, where Indian states or union territories operate independently. The second is an interconnected grid system, where the Indian grid is divided into nine sub-grids linked via high-voltage direct current transmission lines (HVDC TLs). For both case studies, optimal investments are determined using a novel linear optimization approach called Graph-Based Optimization Modeling Language (GBOML). Furthermore, a global electricity grid (GEG) model is developed to connect high-RE countries through HVDC TL and assess the benefits of cross-border interconnections. The proposed work stands out by addressing key aspects of future energy systems, including sub-grid identification and HVDC TL cost analysis. Moreover, the thermal transmission line loss and the costs associated with converters and HVDC TL for both the Indian grid and the GEG are evaluated to assess its techno-economic feasibility of GEG. Finally, the Weibull distribution parameters for all locations were determined using classical methods and a metaheuristic algorithm. For the Indian isolated grid system, the total annual cost to meet the load demand is INR 22,30,671.12 crores, whereas for the interconnected grid system, it is INR 8,46,808.22 crores. In the GEG, the total cost of overhead line (OHL) is INR 110.63 crores per MW, whereas the cost of underground cables is INR 30.72 crores per MW.

Keywords Global electricity grid · Solar PV · Wind energy · Battery storage system · HVDC TL · GBOML

1 Introduction

Achieving net-zero greenhouse gas emissions (GHGE) by 2100 is essential to limit the global temperature rise to below 2 °C above preindustrial levels. Early progress toward net-zero in several developed regions demonstrates the feasibility of this global target and highlights the importance of proactive strategies. In this study, we develop a comprehensive road map for India to achieve net-zero GHGE by 2050 in a sustainable manner. The approach employs detailed modeling of energy system transformation, cross-sectoral integration, and technology adoption, while also quantifying the associated health co-benefits arising from reductions in co-emitted air pollutants.

2 Background

Global electricity demand has been increasing at a rapid pace, growing by over 4% annually, a trend driven by factors such as sustained economic growth, the accelerating pace

✉ Bimal Kumar Dora
bimaldora5@gmail.com

1 Department of Electrical Engineering, Visvesvaraya National Institute of Technology, Nagpur 440010, India

2 Department of Electrical Engineering and Computer Science, University of Liege, 4000 Liege, Belgium

3 Laboratoire de Génie Électrique Et Électrotechnique de Paris, Université Paris-Saclay, CentraleSupélec, CNRS, 91190 Gif-Sur-Yvette, France

4 Laboratoire de Génie Électrique Et Électrotechnique de Paris, Sorbonne Université, CNRS, 75252 Paris, France

Published online: 16 March 2026

of electrification, and the impacts of climate change [1]. This rising demand highlights the urgent need for sustainable energy solutions. Over the past few decades, numerous environmental regulations have been introduced to address climate change and its associated risks. The Fifth Assessment Report [2] by the Intergovernmental Panel on Climate Change highlighted the critical need to reduce greenhouse gas emissions in the coming decades to mitigate the effects of climate change. Building on this foundation, the 2015 Paris Agreement marked a significant global milestone by setting ambitious climate mitigation targets. These objectives aim to limit the rise in global average temperatures to well below 2 °C above preindustrial levels, with a more aspirational goal of restricting the increase to 1.5 °C [3]. Achieving these targets requires coordinated international efforts, significant investments in renewable energy (RE) technologies such as solar photovoltaic (PV) systems and wind energy (WE) systems, and the adoption of innovative strategies to decarbonize energy systems worldwide.

Achieving the policy goal of net-zero greenhouse gas emissions requires the substantial integration of RE, whose immense theoretical potential in decarbonizing the global power system has already been highlighted in numerous studies [4, 5]. However, the practical implementation and reliability of systems with a lot of renewable energy sources (RES) remain subjects of ongoing research due to the inherently intermittent nature of RE technologies. These challenges have initiated growing interest in practical solutions to enhancing RE integration. In view of these, several strategies such as leveraging the complementarity of diverse RES [6], incorporating battery storage systems (BSS) [7], enabling sector coupling [8], and expanding grid infrastructure [9] have been proposed. Moreover, advancements in ultra-high voltage transmission technologies have opened new possibilities for long-distance, transcontinental electricity interconnections [10].

One promising solution to addressing the intermittency of RES is the interconnection of adjacent power systems, allowing the transfer of electricity during periods of surplus or deficit in different zones. By leveraging geographical diversity, this approach smooths out fluctuations in RE production. Expanding on this idea, many ambitious projects have explored the feasibility of interconnecting continental power grids, paving the way for a robust and resilient global energy network [11]. The concept of globally interconnected power grids was first introduced in 2013 by S. Chatzivasileiadis et al. [12], inspired by advancements in electricity transmission technologies that enabled visions of large-scale, cross-border energy networks. This concept envisions a future in which global interconnections facilitate the decarbonization of the electricity sector by enabling the efficient harnessing and sharing of vast RES. Regions with the highest potential for RE generation are often geographically distant from major load centers. Global interconnections can bridge this gap with high-voltage direct current transmission line (HVDC TL) [12]. Such a system could distribute clean electricity across continents, balancing supply and demand on a global scale while contributing to the decarbonization of energy systems worldwide. M. Brinkerink et al. [11] comprehensively reviewed the benefits and challenges of global power grids in 2019. In the same year, CIGRE [13] studied the feasibility of a global electricity network structured into thirteen interconnected regions, highlighting the technical and economic aspects of large-scale energy integration.

2.1 Related works

Numerous studies have investigated electricity interconnections between regions, emphasizing the potential advantages and challenges of creating a global energy system. A. N. Commin et al. modeled Shetland's electricity demand over 30 years using historical meteorological and demand data and compared it to simulated wind power output from various wind farm sizes using the WAsP model [14]. Extensive research has been conducted on connecting Europe with Russia for importing onshore wind and hydro energy from Russia to the EU [15], as well as with the Mediterranean region for importing solar PV from deserts [16]. The Joint Research Centre of the European Commission proposed potential interconnection routes between Europe and China [17] and Europe and Central Asia [18]. Furthermore, researchers have extensively analyzed the benefits of integrating the power grids of Europe and North America [19]. Researchers have explored grid interconnection schemes involving Xinjiang in China, Pakistan in South Asia, and five Central Asian countries [20]. In addition to these efforts, India has also taken initiatives and launched the One Sun, One World, One Grid project to boost up the concept of the global electricity grid (GEG). A prominent example of regional interconnection is the Euro-Asia Interconnector, which is under construction to link Israel, Cyprus, and Greece [21]. In the USA, the National Renewable Energy Laboratory (NREL) conducted the "Interconnections Seam Study," evaluating the benefits of increasing HVDC capacity between Eastern and Western power grids [22]. Following the 2015 Paris Agreement, countries worldwide have been accelerating the expansion of their RE capacity, aiming to meet 80% to 100% of their electricity demand from renewable sources by 2050 [23].

In 2024, P. Arevalo et al. [24] proposed an optimized electrical system for Ecuador in 2050, employing a neuro-fuzzy adaptive inference system to forecast electricity demand using real historical data. In the same year, S. Behera et al. [25] successfully developed and implemented a Feed-in Tariff strategy within an inertia-based generation and transmission expansion planning optimization framework on the IEEE test system. Meanwhile, R. Molu et al. [26] evaluated a

Table 1 Details of literature survey

Ref	Grid expansion region	Sub-grid location identified?	Cost analysis of cross-border HVDC TL	Cost analysis of HVDC TL within a country	Optimal RE cost analysis of individual country	Comparing cost for isolated grid and interconnected grid
[9]	Europe	Yes	No	No	No	No
[11]	Global	No	No	No	No	No
[12]	Global	Yes	Partly Done	No	No	No
[13]	Global	Yes	No	No	No	No
[15]	Global	Yes	Yes	No	No	No
[16]	Europe and Russia	Yes	No	No	No	No
[17]	Europe, North Africa, and the Middle East	Yes	No	No	No	No
[18]	Global	Partly	No	No	No	No
[19]	Central Asia and Europe	Yes	No	Yes	No	No
[20]	Europe and North America	Yes	No	No	No	No
[21]	Central Asian countries	Yes	No	No	No	No
[23]	USA	Yes	No	Yes	No	No
[31]	Global	Yes	Yes	No	No	No
our work	Global	Yes	Yes	Yes	Yes	Yes

novel hybrid PV/diesel/generator energy system for Douala, Cameroon, using HOMER Pro to analyze load demands, pricing models, and overall system performance. Building on these advancements, recent studies have focused on integrating RES with electric vehicles to design more efficient hybrid energy systems [27, 28]. Extending this trend, in 2025, M. Bilal et al. [29] designed and sized standalone microgrids combining renewable energy sources, diesel generators, and battery storage, while also incorporating environmental considerations, highlighting the growing emphasis on sustainable and resilient energy solutions. In addition, a study was conducted on the cost-effective optimization of on-grid electric vehicle charging systems integrated with renewable energy and energy storage. This work presents an economic and reliability analysis using an improved salp swarm algorithm [30].

Table 1 presents the key findings of the literature survey done in this work. While most studies focused on Europe, Central Asia, or had a global perspective, few identified specific sub-grid locations or conducted detailed cost analyses. Only a limited number of them, such as [19] and [23], analyzed the cost of HVDC TL within a country, with [19] being the only one among them to evaluate cross-border HVDC TL costs. None of the referenced works assessed the optimal RE cost at the individual country level or compared the costs of isolated versus interconnected grids. In contrast, the proposed work stands out by comprehensively addressing all critical aspects of sub-grid identification, cost analysis of both domestic and cross-border HVDC TLs, optimal RE cost evaluation for individual countries, and a comparative analysis between isolated and interconnected grid configurations, thereby filling important research gaps in existing literature.

The GEG refers to an intercontinental network of interconnected power systems that enables the seamless exchange of electricity across multiple countries and regions worldwide. It is built on three key pillars: RE capacity expansion, interconnection of nations, and cross-border energy trading [31]. To date, some research has been conducted on RE site selection and capacity expansion to maximize achievable RE generation. Additionally, some studies have explored cross-border energy trading with neighboring countries.

2.2 Contribution

In this study, a detailed analysis is conducted to determine the optimal installation and operation and maintenance (O &

M) costs associated with solar PV, WE, and BSS for isolated grid and when these grids are interconnected to demonstrate the benefits of an interconnected grid. In this paper, three case studies are analyzed to evaluate different grid configurations and their investment requirements. The first case study considers an isolated grid system, where individual Indian states or UTs operate independently without interconnections. The second case study examines an interconnected grid system, in which the national grid is divided into nine subgrids that are interconnected through HVDC TL. For both of these scenarios, optimal investment strategies are determined using a novel linear optimization framework, the Graph-Based Optimization Modeling Language (GBOML), which enables systematic assessment of renewable integration and cost minimization. Furthermore, a novel GEG model is proposed, and the cost and thermal loss associated with HVDC TL are calculated, providing valuable insights into the feasibility of large-scale energy interconnection. Previous studies on formulating the GEG have primarily focused on the shortest distance between two points and calculated their distance considering the exact straight-line distance between coordinates as the transmission distance. However, this approach often requires extensive underwater transmission, which is not cost-effective. In contrast, this study prioritizes the use of more OHL to enhance cost efficiency. Furthermore, to make the analysis more realistic, a 20% leverage factor is applied to the transmission distance, accounting for practical routing constraints and real-world implementation challenges. In this study, mainly three case studies are taken into account and discussed below.

The primary contributions of the proposed work are:

- The total load demand of each Indian state and Union Territory is primarily met using local solar PV, WE, and BSS and calculates the optimal installation, O&M, and energy importation costs using the GBOML.
- The Indian interconnected grid system is developed and modeled using GBOML to calculate the optimal installation, O&M cost, and energy importation cost.
- To compare the isolated grid system and interconnected grid system, the cost and loss associated with HVDC TL are also included in the interconnected grid system.
- The GEG is developed by subdividing the world into 24 main grids, and the rest of the neighboring countries are interconnected to the neighboring main grid.
- For the GEG, the cost and loss associated with HVDC TL are determined.

2.3 Paper organization

The rest of the paper is structured as follows: Sect. 2 provides the information about the wind, solar, and load data extrapolation. Section 3 gives an overview of the design of the isolated grid, the Indian grid, and the GEG. Section 4 discusses the problem formulation, while Sect. 5 focuses on the design and implementation of GBOML. Section 6 presents and analyses the simulation results. Finally, Sect. 7 summarizes the key findings and concludes the work.

Table 2 Installation and O & M cost of various technology type

Technology	Installation Cost (Cr INR per MW)	O & M Cost (Cr INR per MW)	Lifetime (Years)
Solar PV	5.46	0.091	25
Onshore wind	11.284	0.273	25
Battery	1.365	0.2275	15
Distribution grid	0.000455	Included	NA

2.3.1 Data extrapolation

In this study, solar PV power is calculated using a range of meteorological and operational data. For the solar PV power analysis, key parameters including global horizontal irradiance (GHI), diffuse horizontal irradiance (DHI), direct normal irradiance (DNI), zenith angle, azimuth angle, and air temperature for all states and UTs were obtained from the Solcast dataset [32]. Additionally, relative humidity, surface pressure, and wind speed (WS) for these regions were collected from the MERRA2 database [33] for wind power calculations. Hourly load data for all states and UTs were sourced from the India Climate & Energy Dashboard dataset [34]. To determine the capacity factor (CF) for WE, the Suzlon S144 3 MW Series wind turbine was taken into account. This turbine has cut-in and cut-out WS of 3 m/s and 18 m/s, respectively. It has a rated WS of 9.2 m/s. Its rotor diameter is 144 m, and its rated capacity is 3 MW [35]. The load demand data for all the states and UTs are taken from the India Climate & Energy Dashboard. The investment cost, O & M costs, and lifetime of each technology used in this analysis were extracted from [36]. The investment cost and O & M costs are converted from EURO to INR at an exchange rate of 91 INR per EURO as in February 4, 2025, and presented in Table 2. In this study, the cost of TL and converters and losses in TL and converters are taken from [23]. In this study, a GEG is developed with 100% renewable energy generation to support the achievement of the United Nations' Net-Zero 2050 target. Furthermore, the cost of TL and converters is converted from USD to INR at an exchange rate of 87 INR per USD as in February 4, 2025, and presented in Table 3.

Table 3 Installation cost of HVDC TL type

HVDC Type	TL cost (INR per MW.km)	Converter pair cost (Cr INR per MW)	TL loss per 1000 km (%)	Converter pair loss (%)
± 800 kV OHL	8,613	1.9836	2.79	1.4
± 800 kV USC	76,125	1.9836	1.6	1.4
± 1100 kV OHL	12,354	1.7574	1.6	1.4

2.3.2 Grid design

In this work, three case studies are considered. In the first case study, all the states and UTs of India except Lakshadweep and Andaman and Nicobar Islands are treated as isolated/individual grid systems. In the second case study, an Indian interconnected grid system is developed to examine whether the interconnection is economically viable. Furthermore, in the interconnected grid system, an HVDC TL is also incorporated for practical analysis. Finally, after verifying the effectiveness of the interconnected grid, a GEG is developed. In this section, the detail of grid design is discussed.

Case Study 1: Single grid for each Indian state and UTs In this case study, each state in India is designed as an individual grid. The load demand of each individual states and UTs of India except Andaman and Nicobar Islands and Lakshadweep is primarily managed using solar PV and WE within that respective state or UTs. To balance energy surplus and deficit, BSS is incorporated. When RE generation exceeds the load demand, the BSS switches to charging mode, and when RE generation falls below the load demand, the BSS switches to discharging mode. However, RE sources are intermittent by nature, and load demand is also unpredictable. Sometimes, with solar PV, WE, and BSS, it is still impossible to meet the load demand. During such periods, an emergency grid is connected to compensate for the energy deficit. In this study, the optimal capacity of solar PV, WE, and BSS is determined to minimize both the investment and O & M cost of meeting the load demand. The single grid design is presented in Fig. 1.

In this case study of the single grid system, the main optimization problem is subdivided into a number of sub-optimization problems which are called nodes in the context of GBOML. The first node models the solar panels, the second node models the WE system, and the third node captures the dynamics and costs of the BSS, reflecting the power flows during charging and discharging. The fourth node simulates the consumer load, and the fifth node represents the emergency grid consisting of mostly thermal and hydropower. The power balance between the generation and demand is managed through hyperedges, which interconnect all the nodes in this system.

Case Study 2: Indian grid system In this case study, the main Indian grid is subdivided into nine sub-grids, each located in a specific state or UT, which are interconnected via HVDC TL. The remaining states and UTs are then linked to their respective neighboring sub-grids. The sub-grids division is based on the load demand and population of the states or UTs, and consideration is also given to whether it is a strategically suitable location that allows an easy interconnection with many neighboring states or UTs inside each sub-grid.

This interconnection ensures mutual support between all the states and UTs, facilitating efficient energy sharing. Initially, each state and UT load demand is supplied exclusively by its own solar PV and WE generation. When RE generation exceeds the load demand in one state or UT, the surplus generation is supplied to the corresponding sub-grid. Then the excess power is distributed to the other main grid. If there is still any remaining surplus, it is used to charge the BSS. If any sub-grid experiences an energy deficit, it can draw power from the BSS. Furthermore, if the BSS is unable to meet the power deficit, energy can be imported from the emergency grid. The Indian grid design is presented in Fig. 2.

Case Study 3: Global electricity grid system On earth, the tropical zone is ideal for solar PV generation, while the temperate zone is best suited for WE generation. Furthermore, at times, there may be surplus energy generation, which will be wasted if not stored, and at other times, a Dunkelflaute event may occur when both solar PV and WE generation are significantly low. Therefore, this case study formulates a GEG to facilitate a more efficient and sustainable energy system. The proposed GEG significantly reduces the cost of energy generation, facilitates the effective utilization of surplus renewable power, and ensures energy accessibility for regions with limited renewable energy potential by enabling cross-border electricity support from resource-abundant countries. Therefore, this case study interconnects all countries worldwide through HVDC TL, creating a single, large grid known as the GEG. The GEG, akin to the Indian Grid, divides into 24 main energy hubs, each situated in a different country. The remaining countries are connected to these twenty main grids. This study focuses only on interconnection costs, including converter costs and HVDC TL costs, while assuming that all countries are independently developing their internal grids, as described in Case Study 2. The GEG model is illustrated in Fig. 3.

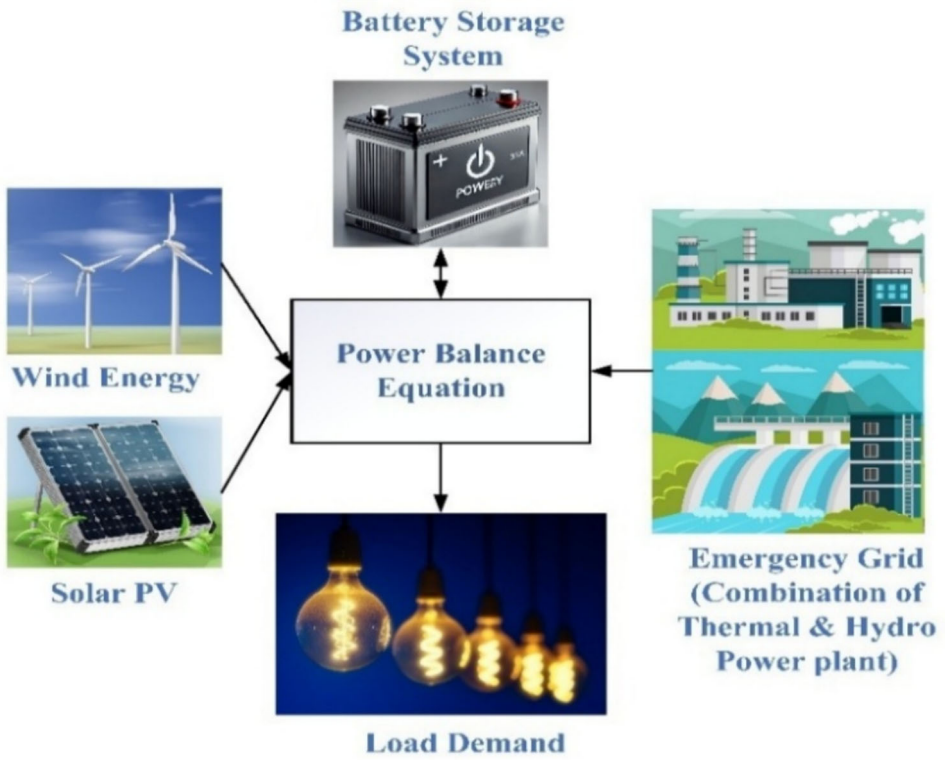

Fig. 1 Single grid system

3 Problem formulation

In this section, the annualized capital expenses (ACEs) for all technologies are first formulated, followed by the analysis of the Weibull distribution (WD) for wind speed characterization. Subsequently, the RE components, such as solar PV and WE systems, are mathematically modeled, and the optimization function is developed. Moreover, the optimization problems for the BSS and the backup grid are also formulated to ensure system reliability and cost-effectiveness.

3.1 Annualized capital expenses

Renewable energy projects typically require a high initial capital investment but benefit from relatively low O & M costs throughout their lifespan. Various energy sources have different lifespans and financing structures, which significantly impact their long-term economic feasibility. To enable a fair comparison of costs across different energy sources, investors often annualize capital expenses, providing a more standardized and accurate assessment of cost-effectiveness. This process is also essential for calculating the levelized cost of energy, a key metric that determines the overall affordability, viability, and competitiveness of a RE project in the energy market. The ACE can be defined as the product of the technology investment cost to produce 1 MW power and the capital recovery factor (CRF) [37].

$$CRF = \frac{r(1+r)^n}{(1+r)^n - 1} \tag{1}$$

where r represents the interest rate and n represents the technology lifetime.

3.2 Weibull distribution

A number of statistical distributions, including the Rayleigh and WD, are used to analyze and characterize WS data and solar irradiance data. However, out of all these statistical techniques, the WD proved to be accurate in fitting and capturing the features of typical changes in WS and solar irradiance [38]. The RE potentials at the chosen locations were analyzed in this research using the Weibull probability density function. The WD represents a specific example of the two-parameter Gamma distribution.

$$P(W) = \left(\frac{k}{c}\right)\left(\frac{W}{c}\right)^{k-1} \exp\left[-\left(\frac{W}{c}\right)^{k}\right] \tag{2}$$

$$F(W) = 1 - \exp\left[-\left(\frac{W}{c}\right)^{k}\right] \tag{3}$$

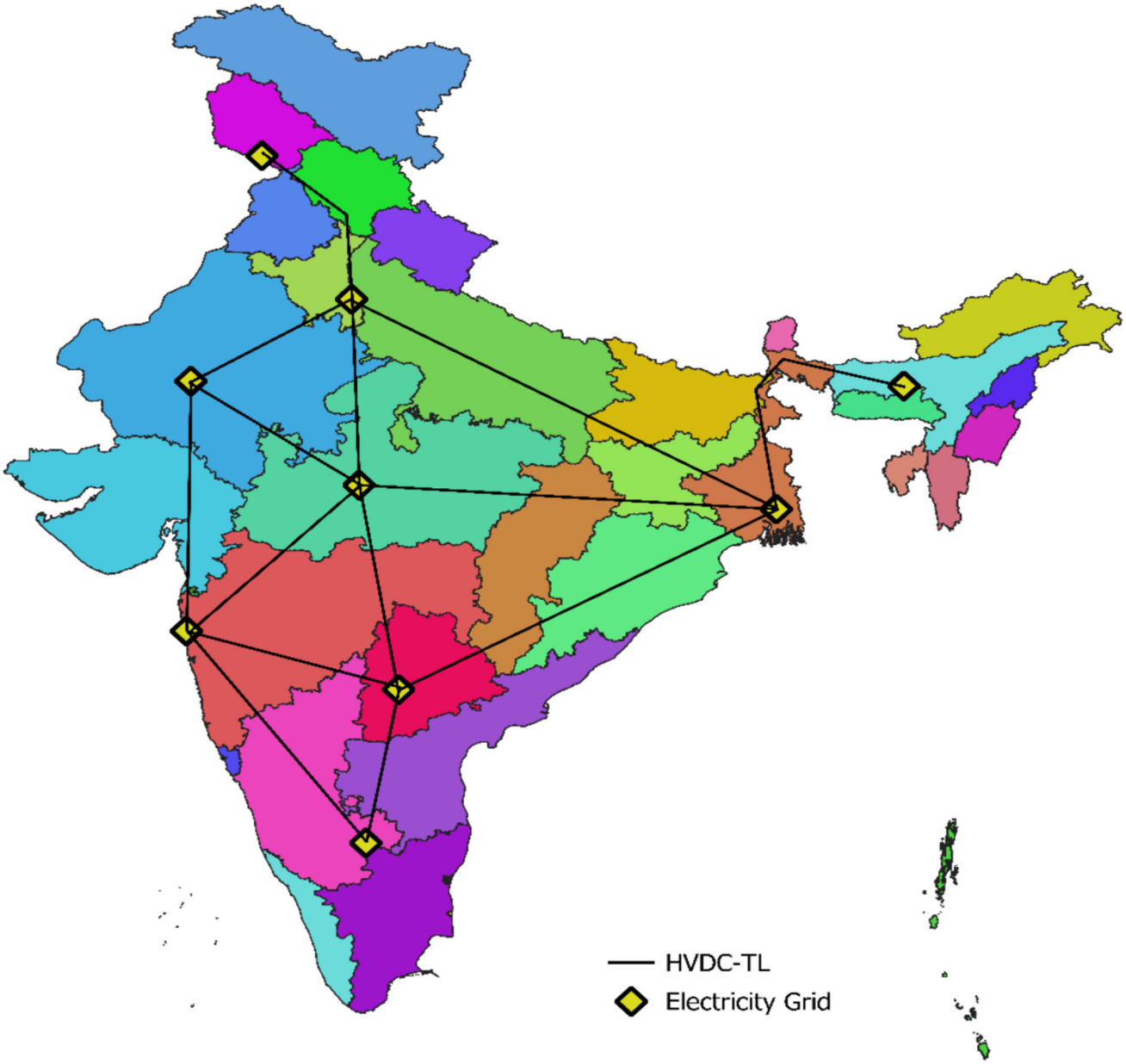

Fig. 2 Indian grid system

where W represents the resultant velocity of the wind or the solar irradiance of the location, k and c represent the shape factor and scale factor, respectively.

It is necessary to know two parameters, k and c, in order to use the Weibull probability density function (PDF). In this paper, various classical techniques such as the energy pattern factor method (EPFM) [39], the empirical method (EM) [40] and the maximum likelihood method (MLM) [39] are employed in order to determine the value of k and c in WD. Recently, various studies have been conducted to estimate Weibull parameters using metaheuristic algorithms. In this study, a newly developed algorithm, the mutualism phase-based Pelican optimization algorithm (MPOA) [40], is implemented to evaluate the values of k and c for all the locations. To select the most accurate Weibull fitting method for obtaining reliable estimates of solar irradiance and WS, root mean square error (RMSE) and the coefficient of determination (R^2) are considered as evaluation metrics [41]. WD can be determined by its probability density function P(W) and cumulative distribution function F(W). The P(W) and F(W) can be mathematically formulated as,

$$RMSE = \frac{1}{N_0 - n} \sum_{a=1}^{n} (y_a - x_a)^2 \tag{4}$$

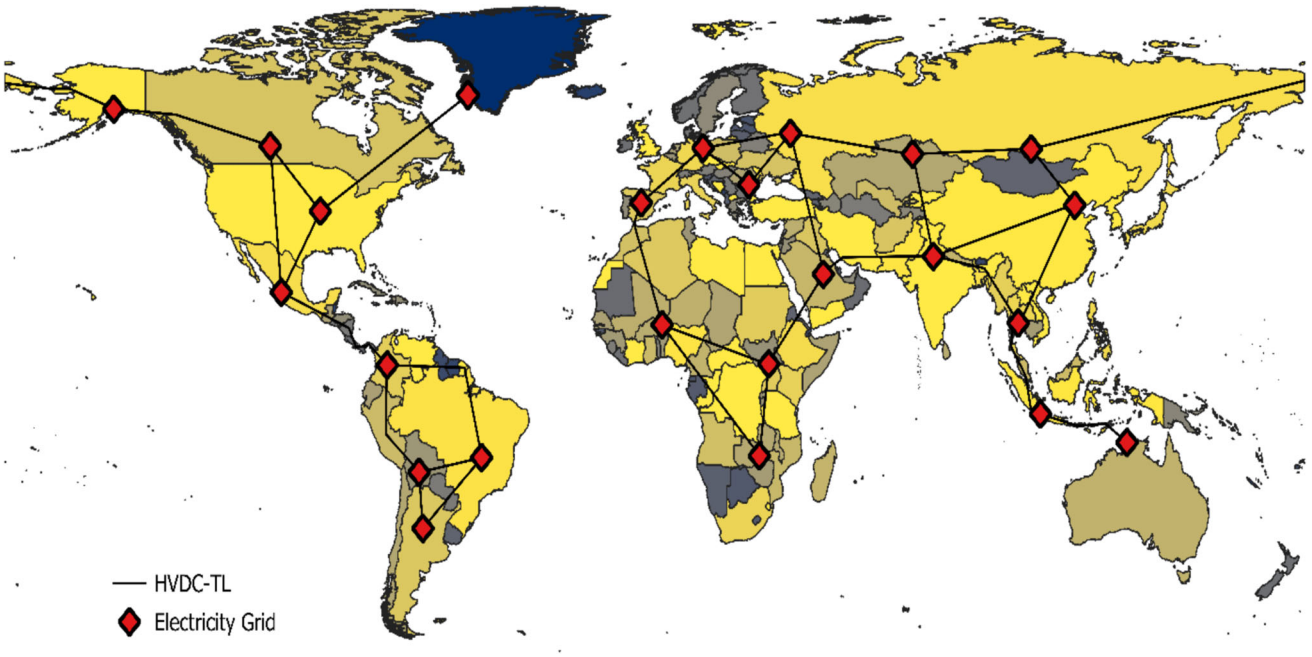

Fig. 3 Global electricity grid system

$$R^2 = \frac{\sum_{a=1}^{n}(y_a - M)^2 - \sum_{a=1}^{n}(x_a - M)^2}{\sum_{a=1}^{n}(y_a - M)^2} \tag{5}$$

where y_a represents the observed value at the a^{th} data point, while x_a denotes the corresponding predicted value. n represents the total number of data points, N_0 represents total number of observations in the dataset, and M represents the average of the observed values y_a.

3.3 Solar PV

3.3.1 Solar power generation

Solar radiation on a surface with an optimal orientation and inclination can be significantly higher than that on a horizontal plane [42]. In India, due to its geographical location and solar trajectory, the irradiance measured on a south-oriented tilted surface remains higher than that on a horizontal plane throughout the day. However, in the early morning hours, the irradiance on an east-oriented tilted surface can be nearly twice as high as that on a south-oriented tilted surface. Therefore, in this study, global tilted irradiance (GTI) is calculated. The GTI is modeled as a combination of three components: DHI, DNI, and GHI. GTI for location l at time t can be mathematically formulated as [43]:

$$R_b = \cos(\theta_z) \tag{6}$$

$$R_d = \left(\frac{1+\cos(\beta)}{2}\right) \tag{7}$$

$$R_r = \left(\frac{1-\cos(\beta)}{2}\right) \tag{8}$$

$$GTI(l,\ t) = DNI(l,\ t) \times R_b + DHI(l,\ t) \times R_d + GHI(l,\ t) \times R_r \tag{9}$$

where Θ_Z and β represent the zenith angle and tilt angle, respectively.

The electrical power generation from the solar PV panel depends on the module temperature and GTI. The electrical power that can be produced from the solar PV for location 'l' at time 't' can be mathematically formulated as [44]:

$$\eta_T(l,\ t) = \eta_{STC} \times [1 - \Upsilon \times (T_{PV}(l,\ t) - T_{STC})] \tag{10}$$

$$P_{PV}(l,\ t) = GTI(l,\ t) \times A \times \eta_T(l,\ t) \tag{11}$$

$$T_{PV}(l,\ t) = T_{air}(l,\ t) + \left(\frac{NOCT - T_{amb}(l,\ t)}{800}\right) \times GTI(l,\ t) \tag{12}$$

where T_{PV}, T_{air}, T_{amb}, and T_{STC} represent the PV module temperature, air temperature, ambient temperature, and PV thermal module temperature, respectively, A represents the area of the PV panel, $NOCT$ represents the nominal operating cell temperature, η_T and η_{STC} represent the temperature

corrected efficiency and the efficiency at standard test condition, and Υ represents the temperature coefficient of the PV panel.

3.3.2 Capacity factor of solar PV

The capacity factor of solar PV for location *'l'* at time *'t'* can be mathematically formulated as the ratio of the power that can be generated from a solar PV panel for location *'l'* at time *'t'* to the rated power of solar PV panel (P^r_{PV}) [43].

$$CF_{PV}(l,\ t) = \frac{P_{PV}(l,\ t)}{P^r_{PV}(l)} \tag{13}$$

3.3.3 Investment cost of solar PV

The primary objective of this study is to determine both investment and operating costs. The total annual investment cost of solar PV per MW comprises the ACE of solar PV per MW (ACE_{PV}) and the O & M cost of solar PV per MW (OMC_{PV}). The annual investment cost of location '*l*' can be mathematically formulated as:

$$C_{PV}(l) = (ACE_{PV}(l) + OMC_{PV}(l)) \times P^r_{PV}(l) \tag{14}$$

where $C_{PV}(l)$ and $P^r_{PV}(l)$ represent the total annual investment cost and the total installation capacity of solar PV park for location *'l'*, respectively.

The minimization of total cost associated with solar PV can be mathematically formulated as:

$$f_{PV} = \min\left[(ACE_{PV}(l) + OMC_{PV}(l)) \times P^r_{PV}(l)\right] \tag{15}$$

At any given time, the power output of the solar panels is calculated as the product of the installed capacity and the dimensionless capacity factor. This capacity factor is determined based on the solar irradiance at that time and the characteristics of the solar PV technology in use. However, the actual power generation can be deliberately curtailed, leading to an output that is lower than the theoretical maximum. This behavior is represented by an inequality constraint relating the power injected into the grid to the maximum possible generation from the solar panels. The power that can be produced by the solar PV park for location l at time t is always less than the maximum installation capacity. The power that can be produced by the solar PV park for location l at time t can be mathematically formulated as:

$$P_{PV}(l,\ t) = P^r_{PV}(l) \times CF_{PV}(l,\ t) \tag{16}$$

$$P_{PV}(l,\ t) \le P^r_{PV}(l) \tag{17}$$

3.4 Wind energy

3.4.1 Wind power generation

Every location has its distinct humidity, pressure, and temperature, each of which has a significant impact on the air density. Moreover, these factors also depend on the height [45]. Air density significantly impacts location and altitude. Therefore, in this study, the air density at each location is determined at a 100-m height. Hence, the wind power density (WPD) calculation using the standard air density is not the same as the actual value. In the MERRA-2 dataset [33] the pressure at surface level and temperature at 2 m height are reported. The air pressure, temperature, and density for location '*l*', at time '*t*', and at height *'h'* can be mathematically formulated as,

$$p(l,\ t) = p_0\left(1 - \frac{Lh}{T_0}\right)^{gM/R_0L} \tag{18}$$

$$T(h_2,\ l,\ t) = T(h_1,\ l,\ t) + L(h - h_1) \tag{19}$$

$$\rho(h,\ l,\ t) = \frac{p(l,\ t)}{R_{Sp} \times T(h,\ l,\ t)} \tag{20}$$

where p_0 represents the pressure at surface level, L the temperature lapse rate (-0.00976 K/m), h the height in meter for which we seek to determine the pressure, T_0 the sea level standard temperature (288.15 K), g the acceleration due to the gravity (9.80665 m/s^2), M the molecular mass of air (0.02896968 kg/mol), R_L the universal gas constant (8.314462618 J/mol.K), and R_{Sp} the specific gas constant (287.05 J/kg.K).

The process of converting WE into electrical energy essentially consists of two stages: firstly, the kinetic energy that exists in the wind is transformed into mechanical energy, which is then used to drive the shaft of a wind generator. The power coefficient C_p represents the efficiency of converting wind power into mechanical power using the blades. It is defined as the ratio of the mechanical energy collected by the blades to the total kinetic energy in the air entering the blade for the same period of time. The mechanical energy is then transformed into electrical energy using wind generators [46]. At this stage, the effectiveness of conversion is determined by the combined efficiency of the gearbox, generator, and electrical components. The gearbox includes losses due to gear tooth friction and bearing friction. The generator experiences both copper and iron losses. In addition to these losses, converter loss and switch loss are also taken into account at this stage. The wind power for location *'l'* at time *'t'* can be mathematically formulated as:

$$\eta = C_p \times \eta_{GB} \times \eta_G \times \eta_C \tag{21}$$

$$P_W(l,\,t) = \eta \times A \times WPD(l,\,t) \tag{22}$$

$$WPD(l,\,t) = \frac{1}{2}\rho(l,\,t) \times V^3(l,\,t) \tag{23}$$

where η_{GB} represents the efficiency off the gearbox, η_G represents the generator efficiency, η_C represents the component efficiency, A represents the swept area of the WT, and η represents the total efficiency of the WT. According to Lanchester–Betz theory, the maximum power that can be extracted by a WT is 59.3% approximately [47].

3.4.2 Capacity factor of wind energy

The capacity factor of wind production (CF_W) can be mathematically formulated as the ratio of the power that can be generated from a wind turbine at time '*t*' location '*l*' ($P_W(l,t)$) to the rated power that can be produced from that wind turbine (P_W^r) [43].

$$CF_W(l,\,t) = \frac{P_W(l,\,t)}{P_W^r(l)} \tag{24}$$

3.4.3 Investment cost of wind energy

The primary objective of this study is to determine the optimized investment cost of WE systems. The total annual investment cost of WE per MW comprises the ACE of WE per MW (ACE_W) and the O & M cost of WE per MW (OMC_W). The annual investment cost of location *'l'* can be mathematically formulated as:

$$C_W(l) = (ACE_W(l) + OMC_W(l)) \times P_W^r(l) \tag{25}$$

where $C_W(l)$ and $P_W^r(l)$ represent the total annual investment cost and the total installation capacity of WE park for location *'l'*, respectively.

The minimization of total cost associated with wind turbines can be mathematically formulated as:

$$f_W = \min\left[(ACE_W(l) + OMC_W(l)) \times P_W^r(l)\right] \tag{26}$$

At any given time, the maximum power output of the wind turbine is calculated as the product of the installed capacity and dimensionless capacity factor. This capacity factor is determined based on the WS at that time and the characteristics of the wind turbine in use. However, the actual power generation can be deliberately curtailed, leading to an output that is lower than the theoretical maximum. This behavior is represented by an inequality constraint relating the power injected into the microgrid to the maximum possible generation from the solar panels. The power that can be produced by the wind park for location *'l'* at time '*t*' is always less than the maximum installation capacity. The power that can be produced by the wind farm for location '*l*' at time '*t*' can be mathematically formulated as:

$$P_W(l,\,t) = P_W^r(l) \times CF_W(l,\,t) \tag{27}$$

$$P_W(l,\,t) \le P_W^r(l) \tag{28}$$

3.5 Investment cost of battery storage system

The primary objective of this study is to determine the optimized investment cost of BSS. The total annual investment cost of BSS per MW comprises the ACE of BSS per MW (ACE_B) and the O & M cost of BSS per MW (OMC_B) [48]. The annual investment cost of location *'l'* can be mathematically formulated as:

$$C_B(l) = (ACE_B(l) + OMC_B(l)) \times P_B^r(l) \tag{29}$$

The minimization of total cost associated with BSS can be mathematically formulated as:

$$f_B = \min\left[(ACE_B(l) + OMC_B(l)) \times P_B^r(l)\right] \tag{30}$$

The energy that can be stored in BSS for location '*l*' at time '*t*' is always equal to or less than the maximum installation capacity.

$$E_B(l,\,t) \le E_B^r(l) \tag{31}$$

The state of charge (SOC) refers to the remaining energy level in a battery relative to its total capacity, typically expressed as a percentage. It serves as an indicator of how much energy is available for use before the battery is depleted. The energy available in the battery for time $t + 1$ at location l can be mathematically formulated as:

$$E_B(l,\,t+1) = E_B(l,\,t) + \eta E_{B+}(l,\,t) - \frac{E_{B-}(l,\,t)}{\eta} \tag{32}$$

where η represents the efficiency of battery regarding charging and discharging loss. E_{B+} and E_{B-} represent the battery energy charging and discharging.

3.6 Investment cost of emergency grid

In this study, it is assumed that the emergency grid has sufficient capacity to compensate for any amount of energy deficit. The cost incurred to supply 1 MW of power to the grid is denoted as O_G. Accordingly, the total operating cost

of power import for location *'l'* at time *'t'* can be mathematically formulated as:

$$C_G(l) = \sum_{t=1}^{T} O_G \times P_{Dff}(l, t) \tag{33}$$

where $P_{Dff}(l,t)$ represents the power deficit of the grid while supplying the load demand using a solar PV, WE, and BSS.

The minimization of total cost associated with the backup grid can be mathematically formulated as:

$$f_G = \min\left[\sum_{t=1}^{T} O_G \times P_{Dff}(l, t)\right] \tag{34}$$

3.7 Total investment cost

In this paper, the total optimized investment cost of the grid can be determined by the addition of optimized costs obtained for solar PV installation, wind turbine installation, BSS installation, and the energy imported from the emergency grid.

$$TC = C_{PV} + C_W + C_B + C_G \tag{35}$$

$$f = f_{PV} + f_W + f_B + f_G \tag{36}$$

3.7.1 Graph-Based Optimization Modeling Language

Graph-Based Optimization Modeling Language (GBOML) was developed by M. Berger et al. in 2021 to solve mixed-integer linear problems by organizing complex optimization problems into interconnected simple suboptimization problems [49]. GBOML is particularly useful for problems where decisions are made at specific, discrete time and over a finite time horizon. GBOML organizes the optimization problems into blocks, which represent different parts or suboptimization problems. These blocks are related in a hierarchical manner, where some blocks depend on others. This relationship can be depicted using a hierarchical hypergraph, where a node represents a subproblem, and hyperedges show how these suboptimization problems are interconnected. By decomposing a large optimization problem into smaller, more manageable subproblems, GBOML simplifies the overall solution process [48].

In GBOML, the time horizon refers to the total duration over which the problem is considered, and discretized time refers to breaking this time horizon into specific intervals [50]. Each subproblem (node) has its own set of constraints and its own objective function such as minimizing or maximizing the output. The hyperedges not only show relationships between subproblems but also carry constraints for the variables that are shared between nodes, known as external variables. In any optimization problem, equality constraints are treated as critical conditions, since they must be satisfied exactly to ensure feasibility of the solution [51]. In the proposed GBOML framework, these equality constraints are systematically handled through hyperedges, which explicitly represent and enforce the required balance relationships among the connected nodes [49]. These constraints ensure that the subproblems remain connected and collectively contribute to solving the overall optimization problem. In the GBOML framework, the variables are divided into two categories: internal variables and external variables. The internal variables refer to actions that are operated and managed within a node itself, whereas the external variables correspond to actions that are coordinated and executed at the global level across the system. In this study, the internal variables considered are installation capacity, investment cost, energy imported from the backup grid, and energy storage parameters in the case of a BSS. The external variables include electricity generation, power consumption, power imported from the backup grid, and charging/discharging operations in the case of BSS. The flowchart of GBOML implementation in grid system is presented in Fig. 4. The steps for solving the optimization problem using GBOML are discussed below:

Step 1: Import *GbomlGraph.*

In this step, the *GbomlGraph* function is imported from the *gboml* Python module by using the syntax:

from gboml import GbomlGraph

Step 2: Create *gboml* model.

The *gboml* model is created by assigning a time horizon in the *GbomlGraph* function. The syntax to assign the time horizon is:

gboml_model = GbomlGraph(T)

Step 3: Import *nodes* and *hyperedges.*

In this step, all the nodes and hyperedges are imported from the linear optimization problem txt file by using the syntax:

nodes, edges, _ = gboml_model.import_all_nodes_and_edges("problem.txt")

Step 4: Add nodes and hyperedges in *gboml* model.

All the *nodes* and *hyperedges* of the suboptimization problems are assigned in the *gboml* model by using the syntaxes given below.

*gboml_model.add_nodes_in_model(*nodes)*

*gboml_model.add_hyperedges_in_model(*edges)*

Step 5: Update model.

In this step, the *gboml* model is updated by building the model with the syntax given below.

gboml_model.build_model()

Step 6: Solve the model.

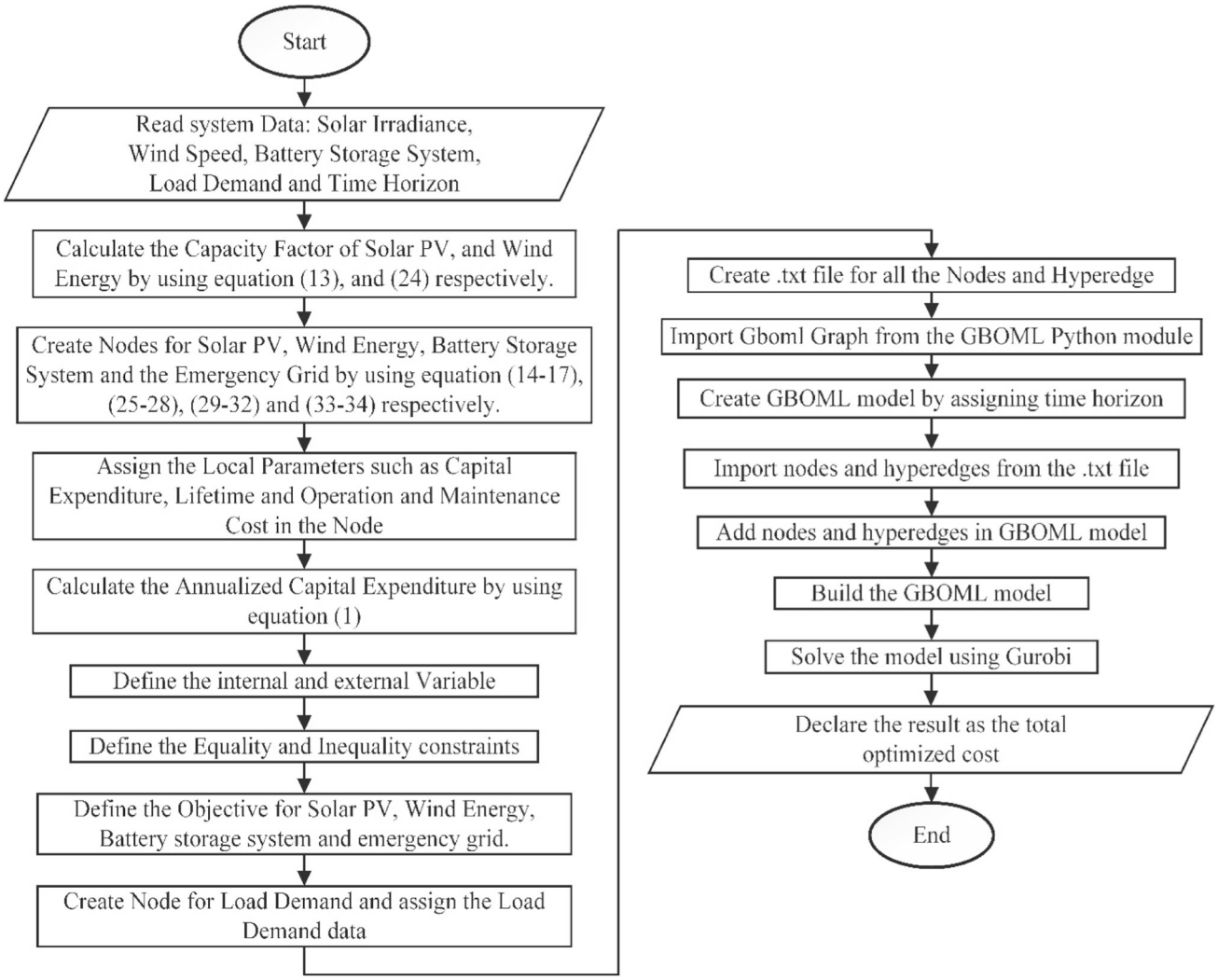

Fig. 4 Flowchart of the implementation of GBOML in grid system

In this study, *gurobi* solver is used to solve the optimization problem. The syntax to solve the optimization problem by *gurobi* is:

solution = *gboml_model.solve_gurobi()*

4 Result analysis and discussion

In this study, GBOML is implemented in the Indian grid system to optimize RE installation costs. The implementation code and associated data are publicly available in a GitHub repository [52]. Solar and wind data are collected from the Solcast dataset and MERRA–2 dataset and analyzed in MATLAB 2023b on a personal computer equipped with an Intel i9 processor (2.50 GHz), 32 GB RAM, a 500 GB SSD, and a 1 TB HDD. GBOML is applied to determine the total optimal RE installation cost using Python 3.12 version and the Gurobi 11.0.3 licensed version. Additionally, the converter cost, HVDC TL cost, and HVDC TL losses are also evaluated for the Indian grid as well as GEG. In this study, HVDC OHL and undersea cable (USC) are used for power transmission. For OHL, an 800 kV TL is selected for distances ranging from 600 to 2600 km, while a 1100 kV TL is chosen for distances beyond 2600 km. For underwater transmission, an 800 kV USC TL is used for power transmission. Finally, the Indian grid system and GEG system are designed with a proper coordinate system in QGIS version 3.34 software.

Case Study 1: Single grid for each Indian state and UTs In this case study, at first, the load demand is primarily managed using solar PV and WE within that respective state or UTs. When these technologies are unable to meet the load demand, an emergency grid with a fixed per-unit price is connected to balance the load, which is also handled by GBOML. The results obtained from the GBOML are presented in Table 3, which shows that the total investment cost required to meet the load demand of all the individual states

and UTs in India separately is INR 22,24,482.38 crores per year for a 10 year period. In addition, some states and UTs in India have low windy areas and unfavorable weather conditions, making them unable to generate sufficient amounts of WE and solar PV power. Therefore, in these regions, emergency grids and BSS must supply a larger share of the energy demand, leading to significantly higher costs. This problem can be handled by an interconnected grid system. The solar PV CF and wind CF profiles of two states named Andhra Pradesh and Arunachal Pradesh are presented in the Appendix section. Therefore, in Case Study 2, all the states and UTs of India are interconnected to each other.

Case Study 2: Indian grid system In Case Study 2, the GBOML is applied to evaluate the optimal installation cost of the solar PV and WE in the Indian Grid system with the help of BSS and the emergency grid. The total installation cost obtained from the GBOML for the Indian grid system is INR 8,46,808.22 crores per year for a 10 year period. It can be observed that the cost assessed by the interconnected Indian grid system is 61.93% lower than the cost incurred when each state independently meets its load demand using local RE generation.

In this case study, the cost of converters and HVDC TL needs to be calculated. The foundation of this study is that all states and UTs of India are interconnected through HVDC TL, enabling efficient energy transfer from one location to another. This interconnection significantly reduces the overall installation cost. The Indian grid is subdivided into nine sub-grids and is interconnected by 14 HVDC TLs. Each HVDC TL is equipped with an 800 kV converter pair, costing INR 1.9836 crores per MW and incurring a transmission loss of 1.4%. Therefore, the total cost of the converter is INR 27.7704 crores per MW, and the total cost required to interconnect the Indian grid system by HVDC TL is INR 10.7112 crores per MW. After considering the HVDC TL cost and converter cost in TL cost, the cost assessed by the interconnected Indian grid system is 51.85% lower than the cost incurred when each state independently meets its load demand using local RE generation. In [53], it was reported that suitable leverage distances for routing power lines typically range between 10 and 25%, highlighting the importance of balancing environmental and engineering considerations during the planning phase. Similarly, other studies [54, 55] indicate that a leverage distance of 15–25% is economically viable. Considering this evidence and to balance both technical feasibility and economic efficiency, a leverage factor of 20% has been adopted in the present study. Table 4 presents the cost of HVDC TL and loss obtained from TL and converters.

Case Study 3: Global electricity grid system In Case Study 3, the GEG is designed and subdivided into 24 sub-grids, which are interconnected by 29 HVDC TLs. The sub-grids are strategically selected to be distributed across 24 countries worldwide, while the remaining neighboring countries are interconnected to the nearest sub-grid. It has been observed from Case Study 2 that the electricity generation cost to supply the load demand while using an interconnected grid system is significantly lower than the cost of producing the same load demand individually. In Case Study 3, the cost of HVDC TL and HVDC TL losses of the designed GEG are calculated. As 24 sub-grids of the GEG are interconnected by 29 HVDC TLs, the system needs 29 converter pairs. In this case study, HVDC OHL and USC are used for power transmission. For OHL, an 800 kV TL is selected for distances ranging from 500 to 2500 km, while a 1100 kV TL is chosen for distances beyond 2500 km. For underwater transmission, an 800 kV USC TL is used for power transmission.

In the proposed GEG, the transmission infrastructure comprises twelve 800 kV and seventeen 1100 kV HVDC TL. Consequently, the system requires twelve 800 kV converter pairs and seventeen 1100 kV converter pairs to facilitate the bidirectional conversion between AC and DC systems at each end of the TL. The total cost required for designing the converter pairs is INR 53.679 crores per MW. In the GEG, the total cost for OHL is INR 1,10,63,78,711.86 per MW, i.e., approximately INR 110.6378 crores per MW, while the USC cost is INR 30,72,83,130 per MW, i.e., approximately INR 30.7283 crores per MW. Therefore, the total cost required to interconnect the GEG system using HVDC TL is INR 1,41,36,61,841.86 per MW, i.e., approximately INR 141.3661 crores per MW. In Table 5, 29 HVDC TLs are selected, and the distances between them are calculated. However, the distances considered are based on the coordinates of the respective locations. To account for practical considerations, a 20% leverage distance is added to each TL. Based on these distances, the appropriate HVDC TL types are selected. Table 6 presents the cost analysis of HVDC TL and total loss obtained from TL and converters for all 29 TL.

4.1 Weibull distribution

In this section, the WD of solar irradiance and WS across all states and UTs of India are analyzed. The k and c parameters are estimated using four methods: EPFM, EM, MLM, and MPOA. In Table 7, the Weibull parameters obtained for solar irradiance are presented. In Table 8, the Weibull parameters obtained for wind speed are presented. To select the most accurate Weibull fitting method for obtaining reliable estimates of solar irradiance and WS, root mean square error (RMSE) and the coefficient of determination (R^2) are considered as evaluation metrics [41]. In Table 8, the RMSE and R^2 values obtained from all four methods are compared. The unit of RMSE is m/sec for wind speed and W/m^2 for solar irradiance, and R^2 is unitless. The results indicate that the MPOA algorithm consistently outperforms all classical approaches, including EPFM, EM, and MLM in 27 locations for solar

Table 4 RE installation cost of all individual grid using GBOML

Sl. No	States and union territories	Total optimized generation cost per year (Cr INR)	Sl. No	States and union territories	Total optimized generation cost per year (Cr INR)
1	Andhra Pradesh	66,534.53	18	Maharashtra	2,06,027.12
2	Arunachal Pradesh	61,88.85	19	Manipur	22,780.19
3	Assam	14,463.06	20	Meghalaya	2,933.61
4	Bihar	46,587.93	21	Mizoram	967.01
5	Chandigarh	2,411.27	22	Nagaland	29,921.62
6	Chhattisgarh	38,833.17	23	Odisha	71,635.92
7	Dadra and Nagar Haveli and Daman and Diu	13,632.73	24	Puducherry	2,753.721
8	Delhi	42,216.77	25	Punjab	88,142.22
9	Goa	3,393.30	26	Rajasthan	90,868.63
10	Gujarat	5,53,415.41	27	Sikkim	685.05
11	Haryana	81,702.79	28	Tamil Nadu	1,07,987.63
12	Himachal Pradesh	75,330.93	29	Telangana	69,969.01
13	Jammu, Kashmir and Ladakh	1,17,796.53	30	Tripura	2,237.91
14	Jharkhand	13,258.47	31	Uttar Pradesh	1,69,430.9
15	Karnataka	65,086.33	32	Uttarakhand	19,675.49
16	Kerala	26,288.72	33	West Bengal	65,056.25
17	Madhya Pradesh	1,12,458.16	Total Cost (Cr INR)		22,24,482.38

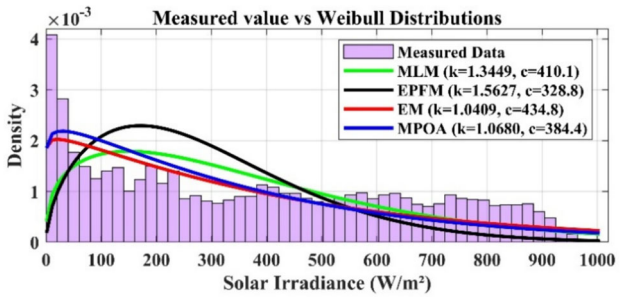

Fig. 5 Measured value vs WD plot of solar irradiance for Andhra Pradesh

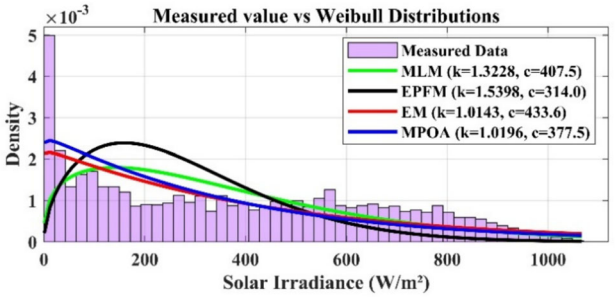

Fig. 6 Measured value vs WD plot of solar irradiance for Arunachal Pradesh

irradiance and 28 locations for WS, respectively. Figures 5 and 6 present the measured values and WD of the solar irradiance plot, while Figs. 7 and 8 show the measured values and WD of the WS plot for Andhra Pradesh and Arunachal Pradesh, respectively. (Table 9).

5 Discussion

The scalability of GBOML represents a critical factor in extending its applicability from localized systems to large-scale interconnected grids. While the framework effectively optimizes installation and operational costs at the state and regional levels, its computational complexity may increase significantly when scaled to national or global systems,

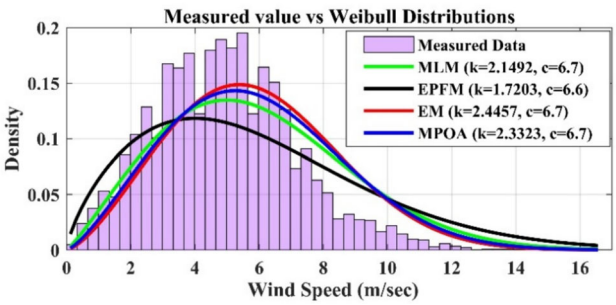

Fig. 7 Measured value vs WD plot of WS for Andhra Pradesh

potentially requiring advanced computational resources. Furthermore, uncertainties in the input data such as fluctuating

Table 5 HVDC TL cost and loss analysis of Indian grid system

State 1	State 2	Distance (km)	Distance (km) + 20%	TL cost (INR per MW)	TL Loss(%)	Total Loss considering Converter Loss (%)
Jammu	New Delhi	510.101	612.1212	52,72,199.8956	1.71%	3.11%
New Delhi	Rajasthan (Jodhpur)	490.169	588.2028	50,66,190.7164	1.64%	3.04%
New Delhi	Madhya Pradesh (Bhopal)	595.686	714.8232	61,56,772.2216	1.99%	3.39%
New Delhi	West Bengal (Kolkata)	1,303.83	1564.596	1,34,75,865.348	4.37%	5.77%
Rajasthan (Jodhpur)	Maharashtra (Mumbai)	796.969	956.3628	82,37,152.7964	2.67%	4.07%
Rajasthan (Jodhpur)	Madhya Pradesh (Bhopal)	553.18	663.816	57,17,447.208	1.85%	3.25%
Madhya Pradesh (Bhopal)	Maharashtra (Mumbai)	661.255	793.506	68,34,467.178	2.21%	3.61%
Madhya Pradesh (Bhopal)	Telangana (Hyderabad)	662.36	794.832	68,45,888.016	2.22%	3.62%
Madhya Pradesh (Bhopal)	West Bengal (Kolkata)	1,123.948	1348.738	1,16,16,680.394	3.76%	5.16%
Maharashtra (Mumbai)	Karnataka (Bengaluru)	844.723	1013.668	87,30,722.484	2.83%	4.23%
Maharashtra (Mumbai)	Telangana (Hyderabad)	617.848	741.4176	63,85,829.7888	2.07%	3.47%
West Bengal (Kolkata)	Telangana (Hyderabad)	1,184.704	1421.645	1,22,44,628.385	3.97%	5.37%
West Bengal (Kolkata)	Assam (Guwahati)	519.177	623.0124	53,66,005.8012	1.74%	3.14%
Karnataka (Bengaluru)	Telangana (Hyderabad)	499.464	599.3568	51,62,260.1184	1.67%	3.07%

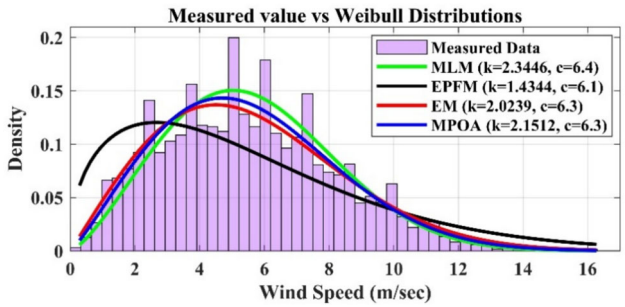

Fig. 8 Measured value vs WD plot of WS for Arunachal Pradesh

renewable generation, load forecasting inaccuracies, and incomplete datasets can influence the robustness of the optimization outcomes, highlighting the need for sensitivity analyses to validate results. In addition, the practical implementation of the GEG presents several challenges beyond technical modeling, including geopolitical cooperation, regulatory harmonization, economic feasibility, and the reliability of long-distance HVDC TL. Addressing these issues is essential for ensuring that the proposed optimization strategies remain realistic, resilient, and adaptable under real-world conditions (Table 10).

6 Conclusions

This study presents a comprehensive assessment of the techno-economic feasibility and structural framework necessary for a large-scale transition to renewable energy (RE) worldwide, along with the formulation of a global electricity grid (GEG). In this study, Graph-Based Optimization Modeling Language (GBOML) is employed to optimize RE installation cost. In Case Study 1, the RE installation costs are calculated for all individual states and union territories (UTs) of India. The total RE installation cost obtained from the GBOML is INR 22,30,671.1178 crores per year. In Case

Table 6 Region distance and HVDC-type selection in global electricity grid system

TL No	Region 1	Region2	Distance (km)		Distance (km) + 20%		HVDC Type
			Land	Sea	Land	Sea	
L1	Berlin, Germany	Moscow, Russia	1608.64	0	1930.37	0	800 kV
L2	Berlin, Germany	Bucharest, Romania	1295.04	0	1554.05	0	800 kV
L3	Berlin, Germany	Madrid, Spain	1869.46	0	2243.35	0	800 kV
L4	Niamey, Niger	Madrid, Spain	3044.66	0	3653.59	0	1100 kV
L5	Juba, South Sudan	Madrid, Spain	5295.31	0	6354.37	0	1100 kV
L6	Lusaka, Zambia	Madrid, Spain	7067.62	0	8481.14	0	1100 kV
L7	Bucharest, Romania	Moscow, Russia	1498.89	0	1798.67	0	800 kV
L8	Juba, South Sudan	Lusaka, Zambia	2272.66	0	2727.19	0	1100 kV
L9	Moscow, Russia	Riyadh, Saudi Arabia	3533.34	0	4240.01	0	1100 kV
L10	Juba, South Sudan	Riyadh, Saudi Arabia	2409.39	324.07	2891.27	388.884	800 kV
L11	New Delhi, India	Riyadh, Saudi Arabia	2741.53	311.3	3289.84	373.56	800 kV
L12	New Delhi, India	Bangkok, Thailand	2926.31	0	3511.57	0	1100 kV
L13	Jakarta, Indonesia	Bangkok, Thailand	2330.58	0	2796.70	0	1100 kV
L14	Jakarta, Indonesia	Darwin, Australia	829.82	1890.49	995.78	2268.588	800 kV
L15	New Delhi, India	Beijing, China	3778.03	0	4533.64	0	1100 kV
L16	New Delhi, India	Astana, Kazakhstan	2555.03	0	3066.04	0	1100 kV
L17	Moscow, Russia	Astana, Kazakhstan	2271.83	0	2726.20	0	1100 kV
L18	Beijing, China	Bangkok, Thailand	3273.96	0	3928.75	0	1100 kV
L19	Beijing, China	Irkutsk, Russia	1656.83	0	1988.20	0	800 kV
L20	Alaska, USA	Irkutsk, Russia	5814.68	0	6977.62	0	1100 kV
L21	Alaska, USA	Saskatchewan, Canada	2718.17	0	3261.80	0	1100 kV
L22	Missouri, USA	Saskatchewan, Canada	1917.73	0	2301.28	0	800 kV
L23	Jalisco, Mexico	Saskatchewan, Canada	3598.18	0	4317.82	0	1100 kV
L24	Missouri, USA	Nuuk, Greenland	3066.43	837.94	3679.72	1005.528	800 kV
L25	Missouri, USA	Jalisco, Mexico	2243.65	0	2692.38	0	1100 kV
L26	Bogota, Colombia	Brasília, Brazil	3663.26	0	4395.91	0	1100 kV
L27	Bogota, Colombia	Sucre, Bolivia	2801.53	0	3361.84	0	1100 kV
L28	Córdoba, Argentina	Sucre, Bolivia	1381.21	0	1657.45	0	800 kV
L29	Brasília, Brazil	Sucre, Bolivia	1873.39	0	2248.07	0	800 kV

Study 2, all states and UTs are interconnected using high-voltage direct current transmission line (HVDC TL), and the total RE installation cost is calculated. The total RE installation cost obtained from the GBOML is INR 8,46,808.2174 crores per year. It can be clearly observed that the total RE installation cost in Case Study 2 of the Indian grid system is significantly lower than that in Case Study 1. In addition, for the Indian grid systems for each HVDC TL, the converter cost, HVDC TL cost, and HVDC TL losses are evaluated. The cost obtained for the converters present in the Indian grid system is INR 27.7704 crores per MW, and the total cost required for the Indian grid system by HVDC TL is approximately INR 10.7112 crores per MW. In Case Study 3, the GEG is proposed, which consists of 24 sub-grids interconnected by HVDC TL, and its converter cost, HVDC TL cost, and HVDC TL losses are evaluated. The cost obtained for the converters present in the GEG system is INR 53.679 crores per MW, and the total cost required to interconnect the GEG system by HVDC TL is approximately INR 141.3661 crores per MW. From this study, it can be observed that considering interconnected multiple grids significantly reduces the RE installation cost, which ultimately provides strong support for the development of the GEG.

6.1 Future scope

In future studies, a similar approach to the Indian grid system can be applied to other countries, structuring their internal energy networks with RE integration. Then the techno-economic feasibility of these national grids can be

Table 7 HVDC TL cost and loss analysis in global electricity grid system

TL No	Installation cost (INR per MW)			TL Loss(%)	Total Loss considering Converter Loss (%)
	Land	Sea	Total Cost		
L1	1,66,26,259.58	0	1,66,26,259.58	5.39	6.79
L2	1,33,85,015.42	0	1,33,85,015.42	4.34	5.74
L3	1,93,21,990.78	0	1,93,21,990.78	6.26	7.66
L4	4,51,36,475.57	0	4,51,36,475.57	5.85	7.25
L5	7,85,01,911.69	0	7,85,01,911.69	10.17	11.57
L6	10,47,76,053	0	10,47,76,053	13.57	14.97
L7	1,54,91,927.48	0	1,54,91,927.48	5.02	6.42
L8	3,36,91,729.97	0	3,36,91,729.97	4.36	5.76
L9	5,23,81,058.83	0	5,23,81,058.83	6.78	8.18
L10	2,49,02,491.28	2,96,03,794.5	5,45,06,285.78	8.69	10.09
L11	2,83,35,357.47	2,84,37,255	5,67,72,612.47	9.78	11.18
L12	4,33,81,960.49	0	4,33,81,960.49	5.62	7.02
L13	3,45,50,382.38	0	3,45,50,382.38	4.47	5.87
L14	85,76,687.592	17,26,96,261.5	18,12,72,949.1	5.05	6.45
L15	5,60,08,539.14	0	5,60,08,539.14	7.25	8.65
L16	3,78,77,808.74	0	3,78,77,808.74	4.91	6.31
L17	3,36,79,425.38	0	3,36,79,425.38	4.36	5.76
L18	4,85,35,802.21	0	4,85,35,802.21	6.29	7.69
L19	1,71,24,332.15	0	1,71,24,332.15	5.55	6.95
L20	8,62,01,468.06	0	8,62,01,468.06	11.16	12.56
L21	4,02,96,326.62	0	4,02,96,326.62	5.22	6.62
L22	1,98,20,890.19	0	1,98,20,890.19	6.42	7.82
L23	5,33,42,298.86	0	5,33,42,298.86	6.91	8.31
L24	3,16,93,393.91	7,65,45,819	10,82,39,212.9	11.27	12.67
L25	3,32,61,662.52	0	3,32,61,662.52	4.31	5.71
L26	5,43,07,096.85	0	5,43,07,096.85	7.03	8.43
L27	4,15,32,121.94	0	4,15,32,121.94	5.38	6.78
L28	1,42,75,634.08	0	1,42,75,634.08	4.62	6.02
L29	1,93,62,609.68	0	1,93,62,609.68	6.27	7.67

analyzed to assess their sustainability. Furthermore, these national grids can ultimately be interconnected to form the GEG, enabling a more resilient, cost-effective, and sustainable global energy network. In addition, many small islands, such as the Andaman and Nicobar Islands and Lakshadweep, are located far from the mainland states and union territories. In these cases, USC transmission is economically unfeasible. Instead, an independent grid system or a multi-island interconnected grid with the nearest islands would be a more cost-effective solution. This also serves as a potential case study for future research. In addition to the areas of future scope discussed earlier, further exploration could focus on dynamic and grid-forming constraints, intra-hour balancing mechanisms, and advanced strategies for enhanced resource integration. In addition, future work could focus on developing an approach that simultaneously optimizes system cost while minimizing CO_2 emissions, thereby achieving both economic and environmental objectives by further reducing the use of backup grid. In future work, a more detailed analysis will be carried out across a wider range between 10 and 90% to determine the optimal leverage distance for each individual route. This extended evaluation will provide deeper insights into route-specific performance and enable more accurate optimization for practical applications.

Table 8 Weibull parameter calculation for solar irradiance

Location	k MLM	c	k EPFM	c	k EM	c	k MPOA	c
Andhra Pradesh	1.3449	410.0875	1.5627	328.7996	1.0409	434.814	1.068	384.3647
Arunachal Pradesh	0.8777	253.5742	0.6104	369.9619	0.5627	231.3958	0.6735	211.8645
Assam	1.2622	381.171	1.4796	263.5308	0.941	401.6281	0.9607	349.1762
Bihar	1.3128	405.6309	1.5256	304.1286	1.0094	428.519	1.0451	379.4438
Chandigarh	1.3053	414.2469	1.5223	306.4834	0.9849	438.1939	1.0245	385.4262
Chhattisgarh	1.3375	418.8441	1.5545	328.8273	1.0323	443.4963	1.0643	392.5905
Dadra and Nagar Haveli and Daman and Diu	1.3125	408.4636	1.5307	308.9004	0.9908	432.5689	1.0275	379.98
Delhi	1.3228	407.5035	1.5398	313.9636	1.0143	433.5832	1.0196	377.5205
Goa	1.3678	441.599	1.6005	368.8032	1.0399	472.7564	1.0318	408.1001
Gujarat	1.3899	450.3839	1.6163	382.6141	1.0976	483.5095	1.0642	418.9839
Haryana	1.3053	414.4975	1.5223	306.6078	0.9847	438.4232	1.025	385.7161
Himachal Pradesh	1.2833	392.1352	1.4853	271.5366	1.0051	411.9223	1.0327	367.1296
Jammu, Kashmir and Ladakh	1.3023	397.7574	1.4959	280.8172	1.0545	417.8841	1.0662	375.0701
Jharkhand	1.3152	411.5938	1.528	308.6358	1.0139	435.0574	1.0462	384.9987
Karnataka	1.4157	463.3293	1.6439	405.2973	1.1583	498.6669	1.0601	429.0633
Kerala	1.3744	441.9579	1.6081	373.2254	1.0482	473.9501	1.0152	405.9731
Madhya Pradesh	1.3256	425.0207	1.5409	323.7715	1.0285	450.4579	1.0349	395.5034
Maharashtra	1.3524	433.2503	1.5742	348.6164	1.0587	462.8623	1.0184	399.5154
Manipur	1.2821	393.0294	1.4967	279.7644	0.9744	413.9147	1.003	364.411
Meghalaya	1.2124	361.5896	1.4263	220.5563	0.9008	376.6833	0.9442	331.9725
Mizoram	1.2592	372.9881	1.4809	260.9589	0.9207	393.5277	0.9472	340.0454
Nagaland	1.2872	382.8236	1.4961	274.6089	0.998	403.3686	1.0205	356.756
Odisha	1.2985	378.522	1.5133	283.3166	0.9868	399.4294	1.0222	352.2967
Puducherry	1.3762	445.4212	1.6016	371.4825	1.0745	475.076	1.0715	416.0151
Punjab	1.322	412.9549	1.5364	314.6417	1.0171	437.7304	1.0437	385.5592
Rajasthan	1.4174	472.829	1.6567	418.4115	1.1185	512.0588	1.0491	436.4886
Sikkim	1.3066	351.3118	1.5112	268.6741	1.0394	374.0103	1.006	324.7949
Tamil Nadu	1.3933	453.9924	1.6235	388.7916	1.0926	486.6915	1.0634	422.0561
Telangana	1.3525	436.0025	1.5772	352.0952	1.0393	464.237	1.0418	405.01
Tripura	1.2674	397.8114	1.4897	277.581	0.9296	367.3765	0.9672	364.9773
Uttar Pradesh	1.3249	412.2875	1.5401	316.5979	1.0202	437.5116	1.0453	384.9703
Uttarakhand	1.2866	395.7089	1.4995	382.7544	0.9742	417.8012	1.0039	366.7398
West Bengal	1.2527	356.7242	1.47	247.1144	0.9317	376.4321	0.9369	324.2717

Table 9 Weibull parameter calculation for wind speed

Location	k	c	k	c	k	c	k	c
	MLM		EPFM		EM		MPOA	
Andhra Pradesh	2.1492	6.6821	1.7203	6.6418	2.4457	6.6722	2.3323	6.6758
Arunachal Pradesh	2.1288	3.9311	2.8353	3.4074	2.8287	3.3762	2.916	3.0988
Assam	2.1288	3.9311	1.2993	3.7692	2.2988	3.8645	2.1286	3.4342
Bihar	1.9934	6.5134	1.2398	6.1863	1.8927	6.5917	1.9957	6.5151
Chandigarh	2.1422	6.3408	1.4733	6.2065	2.0937	6.4461	2.1314	6.3316
Chhattisgarh	1.9868	5.9798	1.186	5.6172	1.9854	6.0393	1.9835	5.9776
Dadra and Nagar Haveli and Daman and Diu	2.1328	6.3936	1.4582	6.2497	2.0803	6.5	2.1228	6.385
Delhi	2.3446	6.3831	1.4344	6.1275	2.0239	6.3116	2.1512	6.2863
Goa	2.189	8.5874	1.4512	8.3885	2.322	8.4639	2.1822	8.5861
Gujarat	2.4019	7.4446	1.82	7.4251	2.4625	7.4941	2.3864	7.437
Haryana	2.1443	6.3391	1.4766	6.2065	2.0944	6.4441	2.134	6.3301
Himachal Pradesh	1.9984	2.3687	1.1734	2.2184	2.0125	2.3517	2.018	5.9344
Jammu, Kashmir and Ladakh	1.9035	3.2292	1.0128	2.3044	2.036	2.5373	1.9309	3.2382
Jharkhand	2.4274	6.518	1.9072	6.5137	2.4176	6.5574	2.4296	6.515
Karnataka	2.5671	7.2466	2.1011	7.2646	2.7192	7.2558	2.5404	7.2363
Kerala	1.8638	5.5508	1.0455	5.0173	1.7804	5.5872	1.8739	5.5583
Madhya Pradesh	2.4582	6.9733	1.9812	6.9774	2.471	7.0718	2.4569	6.9645
Maharashtra	2.2167	7.1853	1.6227	7.1066	2.0803	7.3532	2.2174	7.1779
Manipur	1.5316	2.9996	1.5868	2.9048	1.7551	4.7518	1.6102	3.0319
Meghalaya	2.0419	2.9501	1.1872	2.7707	2.2216	2.8786	2.0557	2.9553
Mizoram	2.1572	6.3554	1.4319	6.1964	2.1632	6.354	2.1589	6.3571
Nagaland	2.064	3.0264	1.2512	2.879	2.18	2.9839	2.0704	3.0291
Odisha	2.1655	5.7178	1.508	7.016	2.0732	7.2572	2.1641	5.7141
Puducherry	2.9334	7.2898	2.9406	7.2891	2.9432	7.3974	2.9692	7.278
Punjab	2.1951	5.5766	1.553	5.4923	2.1567	5.666	2.1869	5.5691
Rajasthan	2.2843	7.8606	1.7501	7.8185	2.1603	8.103	2.2866	7.8486
Sikkim	1.9143	2.4404	1.1323	2.2644	1.7761	2.4509	1.9336	2.4461
Tamil Nadu	2.5244	6.0958	2.0612	6.1071	2.601	6.1297	2.5163	6.0898
Telangana	2.0796	7.1765	1.2849	6.8661	2.1642	7.0476	2.0927	7.188
Tripura	1.9624	4.0367	1.1453	3.756	1.9338	4.0229	1.9776	4.0433
Uttar Pradesh	1.9968	6.187	1.2458	5.8826	1.9215	6.2667	1.9884	6.1816
Uttarakhand	1.8058	3.1271	1.8544	2.7638	2.0306	3.0136	1.8555	3.1426
West Bengal	2.329	6.4948	1.7666	6.465	2.2823	6.5808	2.3327	6.4907

Table 10 Evaluation metrics for Weibull distribution

Locations	Metrics	Solar Irradiance				Wind Speed			
		MLM	EPFM	EM	NMPDOA	MLM	EPFM	EM	MPOA
Andhra Pradesh	R^2	0.3193	0.3790	0.4750	0.5123	0.8943	0.9165	0.9099	0.9270
	RMSE	0.0006	0.0007	0.0005	0.0004	0.0180	0.0140	0.0136	0.0076
Arunachal Pradesh	R^2	0.5685	0.3767	0.8133	0.8462	0.7454	0.8230	0.7612	0.8598
	RMSE	0.0011	0.0013	0.0007	0.0007	0.1420	0.1252	0.1474	0.1011
Assam	R^2	0.4962	0.5207	0.6344	0.7057	0.7872	0.8230	0.8532	0.8864
	RMSE	0.0008	0.0007	0.0006	0.0005	0.0768	0.0252	0.0237	0.0164
Bihar	R^2	0.3377	0.4331	0.5040	0.5351	0.7247	0.8604	0.8496	0.8947
	RMSE	0.0006	0.0008	0.0005	0.0004	0.0292	0.0178	0.0172	0.0075
Chandigarh	R^2	0.6694	0.5064	0.5618	0.6908	0.8858	0.8412	0.8774	0.8505
	RMSE	0.0007	0.0007	0.0005	0.0004	0.0233	0.0467	0.0862	0.0793
Chhattisgarh	R^2	0.5176	0.4608	0.5104	0.4954	0.8458	0.8928	0.8729	0.9085
	RMSE	0.0004	0.0007	0.0004	0.0008	0.0210	0.0144	0.0143	0.0121
Dadra and Nagar Haveli and Daman and Diu	R^2	0.4412	0.4837	0.5476	0.5840	0.8645	0.8804	0.8496	0.8971
	RMSE	0.0007	0.0008	0.0008	0.0005	0.0245	0.0175	0.0170	0.0134
Delhi	R^2	0.3623	0.3027	0.4789	0.5515	0.8738	0.9101	0.9067	0.9375
	RMSE	0.0005	0.0007	0.0005	0.0004	0.0210	0.0159	0.0159	0.0104
Goa	R^2	0.4210	0.4601	0.4497	0.5146	0.8166	0.8701	0.8577	0.8903
	RMSE	0.0008	0.0007	0.0007	0.0006	0.0315	0.0923	0.0849	0.0249
Gujarat	R^2	0.5271	0.5632	0.5286	0.6211	0.8686	0.8704	0.8974	0.9193
	RMSE	0.0007	0.0006	0.0005	0.0005	0.0381	0.0344	0.0479	0.0258
Haryana	R^2	0.4657	0.4359	0.5619	0.6215	0.8994	0.8620	0.8819	0.9064
	RMSE	0.0007	0.0007	0.0005	0.0005	0.0232	0.0367	0.0362	0.0193
Himachal Pradesh	R^2	0.3678	0.4944	0.5359	0.5503	0.9004	0.9365	0.9177	0.9485
	RMSE	0.0005	0.0008	0.0004	0.0004	0.1826	0.3215	0.2609	0.0148
Jammu, Kashmir and Ladakh	R^2	0.4269	0.5577	0.5906	0.5725	0.8784	0.8188	0.8285	0.8691
	RMSE	0.0005	0.0008	0.0004	0.0004	0.1370	0.2471	0.1575	0.1430
Jharkhand	R^2	0.4970	0.5159	0.5891	0.6177	0.8954	0.8545	0.8760	0.9014
	RMSE	0.0006	0.0007	0.0005	0.0005	0.0273	0.0314	0.0213	0.0186
Karnataka	R^2	0.2997	0.3548	0.3105	0.4162	0.9169	0.8955	0.8622	0.9370
	RMSE	0.0007	0.0006	0.0006	0.0005	0.0394	0.0261	0.0354	0.0174
Kerala	R^2	0.4172	0.4541	0.4726	0.5241	0.9180	0.9002	0.8904	0.9269
	RMSE	0.0007	0.0007	0.0006	0.0005	0.0314	0.0376	0.0362	0.0271
Madhya Pradesh	R^2	0.3541	0.4100	0.4751	0.5141	0.8900	0.8603	0.8747	0.9037
	RMSE	0.0006	0.0007	0.0005	0.0005	0.0299	0.0347	0.0319	0.0235
Maharashtra	R^2	0.5431	0.5780	0.6251	0.6513	0.8915	0.8611	0.8364	0.9145
	RMSE	0.0008	0.0007	0.0006	0.0006	0.0253	0.0184	0.0171	0.0162
Manipur	R^2	0.3517	0.4032	0.5642	0.5922	0.9195	0.8968	0.9038	0.9358
	RMSE	0.0007	0.0007	0.0006	0.0005	0.0422	0.0326	0.0352	0.0238
Meghalaya	R^2	0.4086	0.4003	0.4923	0.5305	0.8121	0.8518	0.8314	0.8419
	RMSE	0.0007	0.0007	0.0006	0.0005	0.1406	0.1169	0.2151	0.1296
Mizoram	R^2	0.4003	0.4503	0.5430	0.5503	0.8593	0.8910	0.9104	0.9276
	RMSE	0.0008	0.0007	0.0006	0.0005	0.0203	0.0162	0.0163	0.0118

Table 10 (continued)

Locations	Metrics	Solar Irradiance				Wind Speed			
		MLM	EPFM	EM	NMPDOA	MLM	EPFM	EM	MPOA
Nagaland	R^2	0.4239	0.4612	0.5857	0.6349	0.8425	0.8675	0.8825	0.8946
	RMSE	0.0007	0.0008	0.0007	0.0006	0.1492	0.1768	0.1759	0.1134
Odisha	R^2	0.4206	0.5179	0.5840	0.6225	0.9156	0.9020	0.8930	0.8780
	RMSE	0.0007	0.0008	0.0006	0.0005	0.0093	0.0156	0.0117	0.0188
Puducherry	R^2	0.4884	0.5597	0.5257	0.6075	0.8711	0.9183	0.8926	0.9266
	RMSE	0.0007	0.0007	0.0005	0.0005	0.0393	0.0261	0.0253	0.0190
Punjab	R^2	0.4707	0.5272	0.5821	0.4487	0.8754	0.8320	0.8934	0.9073
	RMSE	0.0005	0.0007	0.0005	0.0006	0.0321	0.0296	0.0250	0.0176
Rajasthan	R^2	0.5033	0.4966	0.6164	0.4147	0.7639	0.8088	0.7754	0.8459
	RMSE	0.0007	0.0006	0.0006	0.0007	0.0443	0.0683	0.0424	0.0368
Sikkim	R^2	0.4517	0.4843	0.5575	0.6136	0.8947	0.8786	0.9133	0.9088
	RMSE	0.0007	0.0008	0.0006	0.0006	0.2346	0.2586	0.0580	0.1683
Tamil Nadu	R^2	0.5160	0.5424	0.4952	0.5873	0.8715	0.8479	0.8194	0.8968
	RMSE	0.0007	0.0006	0.0006	0.0005	0.0235	0.0317	0.0248	0.0190
Telangana	R^2	0.6071	0.5255	0.5450	0.5693	0.9283	0.8928	0.9045	0.9328
	RMSE	0.0005	0.0007	0.0005	0.0005	0.0200	0.0179	0.0224	0.0168
Tripura	R^2	0.5712	0.6156	0.6291	0.6488	0.8282	0.7657	0.7566	0.8580
	RMSE	0.0007	0.0007	0.0006	0.0005	0.0650	0.0447	0.0366	0.0355
Uttar Pradesh	R^2	0.6218	0.7185	0.6781	0.6942	0.8415	0.8848	0.8901	0.9062
	RMSE	0.0007	0.0005	0.0005	0.0005	0.0260	0.0174	0.0170	0.0125
Uttarakhand	R^2	0.5607	0.5213	0.5038	0.5519	0.9063	0.8830	0.8908	0.9150
	RMSE	0.0007	0.0008	0.0005	0.0005	0.1105	0.1364	0.2173	0.0971
West Bengal	R^2	0.5667	0.5351	0.5702	0.6239	0.8382	0.8158	0.8520	0.8762
	RMSE	0.0008	0.0007	0.0006	0.0005	0.0211	0.0152	0.0148	0.0129

Appendix

See Fig. 9

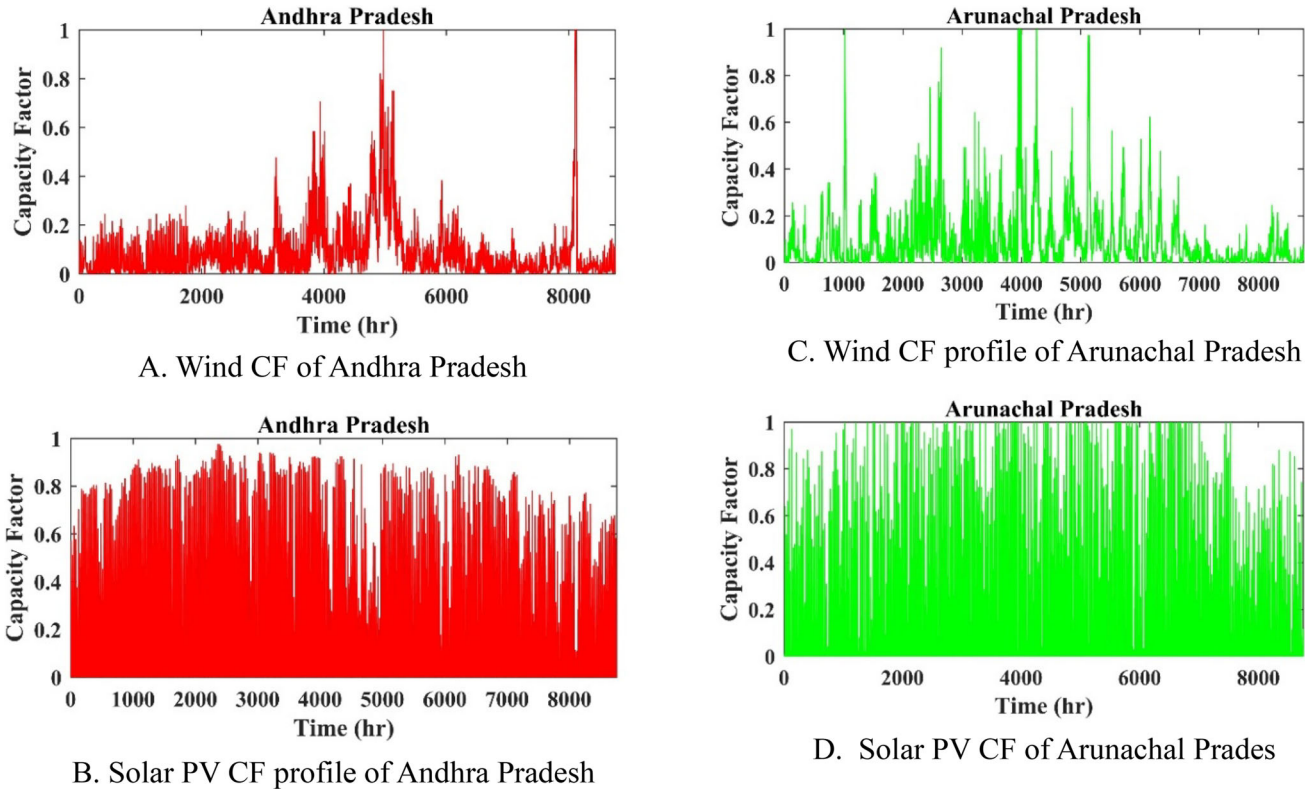

Fig. 9 A. Wind CF of Andhra Pradesh B. Solar PV CF profile of Andhra Pradesh C. Wind CF profile of Arunachal Pradesh D. Solar PV CF of Arunachal Pradesh

Acknowledgements This work is part of the sanctioned project titled "Global Grid: The Future of Earth," funded under the Scheme for Promotion of Academic and Research Collaboration (SPARC) (No. SPARC/2019-2020/P2873/SL, dated 28/07/2023). The authors would like to express their gratitude to the Ministry of Education, Government of India, for their financial support of this project. The authors also sincerely acknowledge Prof. Spyros Chatzivasileiadis (Technical University of Denmark, Denmark) and Dr. Jocelyn Mbenoun (University of Liège, Belgium) for their valuable support and collaboration in this work.

Author contribution B.K.D. conceptualized the study and wrote the main manuscript. S.B., A.M., D.E., and J.D. supervised the work, validated the results, contributed to funding acquisition, and reviewed the manuscript. S.D. and R.F. contributed to data collection, validation, manuscript review, and conceptual development of the work.

Funding Scheme for Promotion of Academic and Research Collaboration, SPARC/2019-2020/P2873/SL, SPARC/2019-2020/P2873/SL, SPARC/2019-2020/P2873/SL, SPARC/2019-2020/P2873/SL, SPARC/2019-2020/P2873/SL.

Data availability No datasets were generated or analyzed during the current study.

Declarations

Competing interests The authors declare no competing interests.

References

1. Pazheri FR, Othman MF, Malik NH (2014) A review on global renewable electricity scenario. Renew Sustain Energy Rev 31:835–845
2. van Ruijven BJ, De Cian E, Sue Wing I (2019) Amplification of future energy demand growth due to climate change. Nat Commun. https://doi.org/10.1038/s41467-019-10399-3
3. McCollum DL et al (2018) Energy investment needs for fulfilling the Paris Agreement and achieving the Sustainable Development Goals. Nat Energy 3(7):589–599. https://doi.org/10.1038/s41560-018-0179-z
4. Davis SJ et al (2018) Net-zero emissions energy systems. Science. https://doi.org/10.1126/science.aas9793
5. DeAngelo J et al (2021) Energy systems in scenarios at net-zero CO2 emissions. Nat Commun. https://doi.org/10.1038/s41467-021-26356-y
6. Bekirsky N, Hoicka CE, Brisbois MC, Ramirez Camargo L (2022) Many actors amongst multiple renewables: a systematic review of actor involvement in complementarity of renewable energy sources. Renew Sustain Energy Rev 161:112368. https://doi.org/10.1016/j.rser.2022.112368
7. Rana MM et al (2023) Applications of energy storage systems in power grids with and without renewable energy integration — a comprehensive review. J Energy Storage 68:107811. https://doi.org/10.1016/j.est.2023.107811
8. Ramsebner J, Haas R, Ajanovic A, Wietschel M (2021) The sector coupling concept: a critical review. WIREs Energy Environ. https://doi.org/10.1002/wene.396

9. Allard S, Mima S, Debusschere V, Quoc TT, Criqui P, Hadjsaid N (2020) European transmission grid expansion as a flexibility option in a scenario of large scale variable renewable energies integration. Energy Econ 87:104733. https://doi.org/10.1016/j.eneco.2020.104733
10. Liu Z, Zhang F, Yu J, Gao K, Ma W (2018) Research on key technologies in ±1100 kV ultra-high voltage DC transmission. High Volt 3(4):279–288. https://doi.org/10.1049/hve.2018.5023
11. Brinkerink M, Ó. Gallachóir B, Deane P (2019) A comprehensive review on the benefits and challenges of global power grids and intercontinental interconnectors. Renew Sustain Energy Rev 107:274–287. https://doi.org/10.1016/j.rser.2019.03.003
12. Chatzivasileiadis S, Ernst D, Andersson G (2013) The global grid. Renew Energy 57:372–383. https://doi.org/10.1016/j.renene.2013.01.032
13. *Power system development and economics C1 Global electricity network Feasibility study*. 2019.
14. Hassan Q, Viktor P, Al-Musawi TJ, Ali BM, Algburi S, Alzoubi HM, Al-Jiboory AK, Sameen AZ, Salman HM, Jaszczur M (2024) The renewable energy role in the global energy transformations. Renew Energy Focus 48:100545
15. Boute A, Willems P (2012) RUSTEC: greening Europe's energy supply by developing Russia's renewable energy potential. Energy Policy 51:618–629. https://doi.org/10.1016/j.enpol.2012.09.001
16. K. Ummel and D. Wheeler, "Desert Power: The Economics of Solar Thermal Electricity for Europe, North Africa, and the Middle East," 2008. [Online]. Available: www.cgdev.org
17. Ardelean M and Minnebo P, "A China-EU electricity transmission link Assessment of potential connecting countries and routes," https://doi.org/10.2760/67516.
18. M. Ardelean, "Optimal paths for electricity interconnections between Central Asia and Europe", https://doi.org/10.2760/95740.
19. Purvins A, Sereno L, Ardelean M, Covrig C-F, Efthimiadis T, Minnebo P (2018) Submarine power cable between Europe and North America: a techno-economic analysis. J Clean Prod 186:131–145. https://doi.org/10.1016/j.jclepro.2018.03.095
20. Huang C, Wang C, Li H, Luo J, Sun W, Du X (2019) Analysis of basic conditions of the power grid interconnection among Xinjiang, Pakistan, and five Central Asian countries. Global Energy Interconnection 2(1):54–63. https://doi.org/10.1016/j.gloei.2019.06.007
21. G. Mitchell, "Supercharged: The EuroAsia Interconnector and Israel's Pursuit of Energy Interdependence," 2021.
22. Bloom A et al (2022) The value of increased HVDC capacity between Eastern and Western U.S. grids: the interconnections seam study. IEEE Trans Power Syst 37(3):1760–1769. https://doi.org/10.1109/TPWRS.2021.3115092
23. Wu C, Zhang XP, Sterling MJH (2021) Global electricity interconnection with 100% renewable energy generation. IEEE Access 9:113169–113186. https://doi.org/10.1109/ACCESS.2021.3104167
24. Arévalo P, Cano A, Jurado F (2024) Large-scale integration of renewable energies by 2050 through demand prediction with ANFIS, Ecuador case study. Energy 286:129446
25. Behera S, Das S, Pardhu BG, Vais RI, Babu NR, Bhagat SK, Alharbi M, Mbasso WF (2024) A comprehensive study on energy management, sensitivity analysis, and inertia compliance of feed-in tariff in IEEE bus systems with grid-connected renewable energy sources. Heliyon. https://doi.org/10.1016/j.heliyon.2024.e36927
26. Molu RJJ, Naoussi SRD, Bajaj M, Wira P, Mbasso WF, Das BK, Tuka MB, Singh AR (2024) A techno-economic perspective on efficient hybrid renewable energy solutions in Douala, Cameroon's grid-connected systems. Sci Rep 14(1):13590
27. Oladigbolu JO, Mujeeb A, Bilal M, Al-Turki YA, Alharbi SS, Alharbi SS (2025) EV charging stations for sustainable urban transport electrification in the Arabian Peninsula: performance assessment, social-economic aspects, opportunities, implementation challenges and strategic policies. Energy Conversion Manage: X. https://doi.org/10.1016/j.ecmx.2025.101018
28. Bilal M, Bokoro PN, Sharma G (2025) Hybrid optimization for sustainable design and sizing of standalone microgrids integrating renewable energy, diesel generators, and battery storage with environmental considerations. Results Eng 25:103764
29. Bilal M, Ahmad F, Mohammad A, Rizwan M (2025) Techno-economic evaluation and sensitivity analysis of renewable energy based designing of plug-in electric vehicle load considering load following strategy. Appl Energy 377:124557
30. Bilal M, Oladigbolu JO, Mujeeb A, Al-Turki YA (2024) Cost-effective optimization of on-grid electric vehicle charging systems with integrated renewable energy and energy storage: an economic and reliability analysis. J Energy Storage 100:113170
31. Dora BK et al (2025) The global electricity grid: a comprehensive review. Energies 18(5):1152. https://doi.org/10.3390/en18051152
32. "Solcast: https://www.solcast.com/."
33. "MERRA-2: https://disc.gsfc.nasa.gov/datasets/M2I1NXASM_5.12.4/summary."
34. "India Climate & Energy Dashboard:
35. https://iced.niti.gov.in/energy/electricity/distribution/national-level-consumption/load-curve."
36. "Suzlon powering a Greener Tomorrow : https://www.suzlon.com/in-en/energy-solutions/s144-wind-turbine-generator."
37. Johansson V, Göransson L (2020) Impacts of variation management on cost-optimal investments in wind power and solar photovoltaics. Renew Energy Focus 32:10–22. https://doi.org/10.1016/j.ref.2019.10.003
38. Yang H, Wei Z, Chengzhi L (2009) Optimal design and techno-economic analysis of a hybrid solar-wind power generation system. Appl Energy 86(2):163–169. https://doi.org/10.1016/j.apenergy.2008.03.008
39. Bagiorgas HS, Mihalakakou G, Rehman S, Al-Hadhrami LM (2016) Wind power potential assessment for three buoys data collection stations in the Ionian Sea using Weibull distribution function. Int J Green Energy 13(7):703–714
40. Suzer AE, Atasoy VE, Ekici S (2022) A framework on the investigation of wind characteristics based on Weibull distribution function by comparative scrutiny of estimation methods: application to an airport. Int J Green Energy 19(3):254–269
41. Dora BK, Bhat S, Halder S, Srivastava I (2024) A solution to multi Objective Stochastic Optimal Power Flow problem using mutualism and elite strategy based Pelican Optimization Algorithm. Appl Soft Comput 158:111548
42. Alizadeh MJ, Kavianpour MR, Kamranzad B, Etemad-Shahidi A (2019) A weibull distribution based technique for downscaling of climatic wind field. Asia-Pac J Atmos Sci 55:685–700
43. Sun V, Asanakham A, Deethayat T, Kiatsiriroat T (2020) A new method for evaluating nominal operating cell temperature (NOCT) of unglazed photovoltaic thermal module. Energy Rep 6:1029–1042. https://doi.org/10.1016/j.egyr.2020.04.026
44. Zhang T, Stackhouse PW, Macpherson B, Colleen Mikovitz J (2024) A CERES-based dataset of hourly DNI, DHI and global tilted irradiance (GTI) on equatorward tilted surfaces: derivation and comparison with the ground-based BSRN data. Sol Energy 274:112538. https://doi.org/10.1016/j.solener.2024.112538
45. Xydis G (2013) On the exergetic capacity factor of a wind – solar power generation system. J Clean Prod 47:437–445. https://doi.org/10.1016/j.jclepro.2012.07.014
46. Yang Z, Huang W, Dong S, Li H (2023) Mixture bivariate distribution of wind speed and air density for wind energy assessment. Energy Convers Manag 276:116540. https://doi.org/10.1016/j.enconman.2022.116540
47. Sedaghat A, Hassanzadeh A, Jamali J, Mostafaeipour A, Chen W-H (2017) Determination of rated wind speed for maximum annual

energy production of variable speed wind turbines. Appl Energy 205:781–789. https://doi.org/10.1016/j.apenergy.2017.08.079
48. M. Ragheb and A. M. Ragheb, "2 Wind Turbines Theory-The Betz Equation and Optimal Rotor Tip Speed Ratio." [Online]. Available: www.intechopen.com.
49. B. Miftari, M. Berger, H. Djelassi, and D. Ernst, "Graph-Based Optimization Modeling Language," 2024.
50. M. Berger, A. Bolland, B. Miftari, H. Djelassi, and D. Ernst, "Graph-Based Optimization Modeling Language: A Tutorial," 2021.
51. Miftari B, Berger M, Djelassi H, Ernst D (2022) GBOML: graph-based optimization modeling language. J Open Source Softw 7(72):4158. https://doi.org/10.21105/joss.04158
52. Dora BK, Bhat S, Halder S, Srivastava I (2024) Multi-objective optimal power flow problem using Nelder–Mead based Prairie Dog optimization algorithm. Soft Comput 28(21):12835–12868
53. Dora, B. K. GBOMLmicrogridAndhraPradesh, accessed: 2025–05–16 (2023). URL https://github.com/BimalKumarDora/GBOMLmicrogridAndhraPradesh.
54. Biasotto LD, Becker FG, Nóbrega RAA, Kindel A (2022) Routing power lines: towards an environmental and engineering friendly framework for avoiding impacts and conflicts in the planning phase. Environ Impact Assess Rev 95:106797. https://doi.org/10.1016/j.eiar.2022.106797
55. Zipf M, Kumar S, Scharf H, Zöphel C, Dierstein C, Möst D (2019) Multi-criteria high voltage power line routing—an open source GIS-based approach. ISPRS Int J Geo-Inf 8(8):316
56. Bagli S, Geneletti D, Orsi F (2011) Routeing of power lines through least-cost path analysis and multicriteria evaluation to minimise environmental impacts. Environ Impact Assess Rev 31(3):234–239